Enhanced Room-Temperature Corrosion of Copper in the Presence of Graphene

Feng Zhou,[†,§] Zhiting Li,[†,§] Ganesh J. Shenoy,[†] Lei Li,[‡] and Haitao Liu[†,*]

[†]Department of Chemistry, University of Pittsburgh, Pittsburgh, Pennsylvania 15260, United States and [‡]Department of Chemical and Petroleum Engineering, University of Pittsburgh, Pittsburgh, Pennsylvania 15261, United States. [§]F. Zhou and Z. Li contributed equally to this work.

ABSTRACT This paper reports the enhancement of long-term oxidation of copper at room temperature by a graphene coating. Previous studies showed that graphene is an effective anticorrosion barrier against short-term thermal and electrochemical oxidation of metals. Here, we show that a graphene coating can, on the contrary, accelerate long-term oxidation of an underlying copper substrate in ambient atmosphere at room temperature. After 6 months of exposure in air, both Raman spectroscopy and energy-dispersive X-ray spectroscopy indicated that graphene-coated copper foil had a higher degree of oxidation than uncoated foil, although X-ray photoelectron spectroscopy showed that the surface concentration of Cu^{2+} was higher for the uncoated sample. In addition, we observed that the oxidation of graphene-coated copper foil was not homogeneous and occurred within micrometer-sized domains. The corrosion enhancement effect of graphene was attributed to its ability to promote electrochemical corrosion of copper.

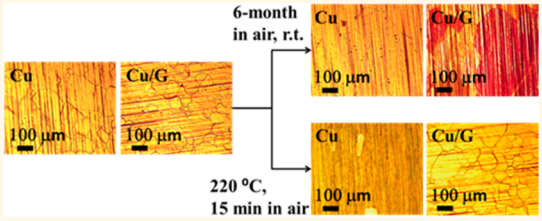

KEYWORDS: graphene · corrosion · oxidation · copper · long-term

Several recent studies have demonstrated that single- and multilayer graphene coatings are excellent anticorrosion barriers for the thermal,[1−8] wet,[1,2,9,10] and electrochemical[11−13] corrosion of metals. Ruoff, Park, and co-workers first reported that a chemical vapor deposition (CVD)-grown graphene can effectively protect Cu and Cu/Ni alloys from thermal oxidation in air at 200 °C for 4 h and wet oxidation by 30% H_2O_2 within 2 min.[1] In a closely related study, Nayak *et al.* reported a similar anticorrosion effect of CVD-grown multilayer graphene for the thermal (500 °C for 3 h) and wet chemical (31% H_2O_2, 2 h) oxidation of Ni.[9] Bolotin and co-workers reported a detailed study of the anticorrosion property of CVD-grown as well as transferred graphene for electrochemical corrosion of Cu and Ni. They observed that graphene films grown on the metal directly by CVD give a better anticorrosion performance than transferred graphene. Nevertheless, even transferred graphene can reduce electrochemical corrosion of Ni by a factor of 4 when compared to the uncoated Ni substrate.[12] A parallel study by Kirkland *et al.* investigated the electrochemical response of graphene-coated Ni and Cu substrates and reached similar conclusions.[11] Roy *et al.* recently explored the use of transferred multilayer graphene coating to reduce thermal oxidation of Cu and concluded that the anticorrosion performance of graphene is ultimately limited by the presence of grain boundaries in graphene as well as its thermal stability in air.[7] In addition to these studies on the anticorrosion application of graphene, the slower oxidation of metal underneath graphene has also been exploited to visualize graphene on copper.[2]

While these studies have firmly established that graphene is a promising anticorrosion material, they exclusively focused on corrosion processes under very harsh conditions over a relatively short time scale, typically several minutes to several hours. Under these conditions, the diffusion of oxidation agents (*e.g.*, O_2 and H_2O_2), instead of their reaction with the metal, is expected to be the rate-limiting step of the overall corrosion process. Indeed, several studies have attributed the anticorrosion property

* Address correspondence to hliu@pitt.edu.

Received for review April 29, 2013 and accepted July 24, 2013.

Published online July 24, 2013
10.1021/nn402150t

of graphene to its capability to serve as an ultrathin physical barrier, preventing direct interaction between underlying metal and ambient oxygen.[1−4,7,8,14,15]

Many technologically relevant corrosion processes (*e.g.*, steel corrosion) occur at room temperature but over a relatively long time scale, from months to years. Under such conditions, the overall corrosion process could be limited by the reaction between the metal and the oxidation agent; as a result, the slower diffusion of oxidation agent through an anticorrosion coating may not help to slow the overall corrosion process. More importantly, electrochemical oxidation plays a significant role for the low-temperature corrosion of metals. It is very well established that the presence of impurities, including graphitic materials, on a metal surface could enhance its galvanic corrosion by serving as an electrode for oxygen reduction.[16−18] Given these considerations, it is not clear if graphene can serve as an effective anticorrosion coating for the long-term protection of metals.

In this work, we show that a CVD-grown graphene coating accelerates the room-temperature, long-term oxidation of copper. By using a combination of Raman spectroscopy, X-ray photoelectron spectroscopy (XPS), and energy-dispersive X-ray spectroscopy (EDX), we show that copper is oxidized faster in the presence of a graphene coating than in its absence. Furthermore, the oxidation is not spatially homogeneous; instead, it occurs in micrometer-sized domains surrounded by areas having minimal oxidation. Our observation suggests that graphene promotes electrochemical corrosion of copper at room temperature.

RESULTS

We studied the oxidation of copper in two types of samples over a time frame of 6 months: a single layer graphene coated copper foil (graphene/copper sample or graphene-coated sample) and a H_2-annealed copper foil (annealed copper sample or uncoated sample). The graphene/copper sample was prepared by a low-pressure chemical vapor deposition method first reported by Li *et al.*[19] A Raman spectrum of our graphene sample is shown in Figure S1. The intensity ratio of the 2D peak to that of the G peak (I_{2D}/I_G) was 4.2, and there was almost no D peak present, indicating the formation of high-quality single-layer graphene. The H_2-annealed copper foil was prepared by processing the copper foil under the same condition as in the case of CVD graphene synthesis except no CH_4 gas was introduced.

Short-Term Anticorrosion Effect of Graphene. We were able to confirm the short-term anticorrosion effect of graphene reported by several recent studies.[1−3] In one experiment, we heated an as-received copper foil (without H_2 annealing) and a graphene/copper sample in air at 250 °C for 20 min. Figure S2 shows the photograph of both samples after the thermal treatment. Annealing the as-received Cu foil led to a loss of its metallic luster and a drastic color change to gray and black, which was attributed to the formation of oxides on its surface.[1] In contrast, after the same treatment, the graphene/copper sample kept its metallic luster and no obvious color change was observed. This result demonstrated that a single-layer graphene coating can indeed effectively prevent atmospheric oxidation of copper at high temperature over a short time frame.

Long-Term Corrosion-Promotion Effect of Graphene. To investigate whether graphene can also serve as an anticorrosion coating over a much longer time scale, a graphene/copper sample and an annealed copper sample were stored in a plastic Petri dish at room temperature (*ca.* 21 °C) for up to 6 months in the dark.

Figure 1 shows the photographs and optical micrographs of a graphene/copper sample and annealed copper sample taken when they were freshly prepared (<1 day) and after 6 months of air exposure. When freshly prepared, both samples showed the characteristic copper luster to the naked eye. When inspected under an optical microscope, both samples appeared to be highly reflective, and when recorded on a digital camera, they appeared to be yellow in color (Figure 1a,d).

After 6 months of storage, the two samples were very different in appearance. The graphene/copper sample developed many millimeter-sized patches in deep brown, red, or yellow colors (Figure 1b, inset). Under an optical microscope (Figure 1b), most (∼90%) of these patches appeared to be red when recorded on a digital camera; a small percentage (∼10%) of the patches appeared to be yellow (*vide infra*). Note that Figure 1b was taken at an area having both red and yellow patches in order to highlight their color contrast; it does not represent their actual surface coverage. Additional micrographs of the two samples can be found in Figure S3. In contrast, the annealed copper foil showed almost no color change to the naked eye, and when inspected under an optical microscope, almost all the surface appeared to be yellow (Figure 1e). However, we could still locate patches that turned a red color. These red-colored patches are similar to those observed in the aged graphene/copper sample, except in this case they cover only *ca.* 1% of the surface. More interestingly, under a higher magnification, we found micrometer-sized red dots or domains on both 6-month-aged samples (Figure 1c,f), suggesting a spatially homogeneous oxidation of copper (*vide infra*).

Previous studies suggested that the color change on the copper surface is related to its degree of oxidation.[1,2] Because a much more drastic color change was observed for the aged graphene/copper sample than for the aged annealed copper sample, our result suggests that, qualitatively, copper was oxidized faster

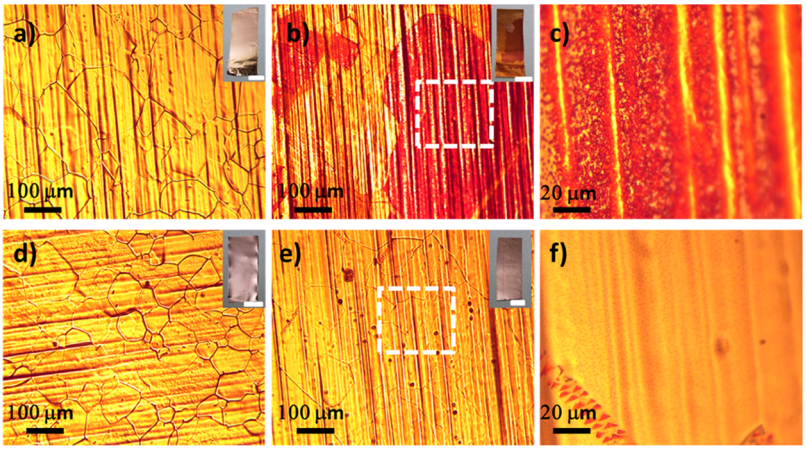

Figure 1. Optical micrographs of (a) an as-prepared graphene/copper sample, (b) a 6-month-aged graphene/copper sample, (d) an as-prepared annealed Cu foil, and (e) a 6-month-aged annealed Cu foil. (c and f) Magnified optical images of the dashed area in (b) and (e), respectively. Insets in (a), (b), (d), and (e) show the photograph of the respective samples. Scale bars in the insets represent 1 cm.

at room temperature in the presence of graphene than in its absence.

To quantify the degree of oxidation of the two 6-month-aged samples, we carried out EDX and Raman analysis on both samples. The result confirms that the graphene-coated sample indeed underwent more severe oxidation than the noncoated one. In the case of EDX analysis, we collected an EDX spectrum from the red-colored regions of a 6-month-aged graphene/copper and the yellow-colored region of 6-month-aged annealed Cu sample. A typical set of EDX spectra are shown in Figure 2a. The average O:Cu atom ratios, obtained from several of such spectra, were 1:17 and 1:13 for aged annealed Cu and aged graphene/copper sample, respectively. Note that EDX probes *ca.* 1 μm thick of sample within the surface.[20] Therefore, it can probe both copper oxides on the surface and the underneath Cu unless the thickness of the oxide layer is significantly larger than 1 μm. The fact that the O:Cu ratio we observed is much lower than that expected for CuO (1:1) and Cu_2O (1:2) indicates that the oxide layer is indeed much thinner than the probe depth of EDX. Nevertheless, a higher O:Cu ratio and a higher absolute intensity of the oxygen EDX peak clearly suggest a higher degree of oxidation in the graphene-coated sample.

In addition to the EDX analysis, Raman spectroscopy of the samples also indicates that the graphene/copper sample underwent a higher degree of oxidation than the annealed copper sample. Shown in Figure 2b are Raman spectra collected from 6-month-aged graphene/copper and annealed copper samples; a spectrum taken from an as-received copper foil that has undergone thermal oxidation at 220 °C for 15 min in air is also shown for reference. All spectra were taken under the same conditions. Both 6-month-aged samples showed Raman peaks that can be assigned to Cu_2O (218 cm^{-1}) and CuO (300 cm^{-1}).[21−24]

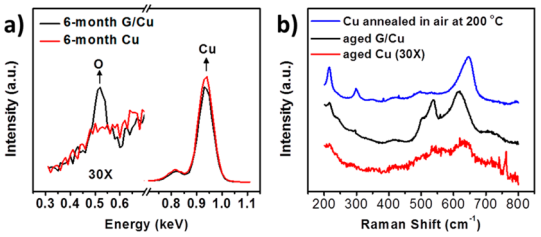

Figure 2. (a) Typical EDX spectra of 6-month-aged graphene/copper (black) and 6-month-aged annealed copper (red) from 0.3 to 1.1 keV. Note that the spectra from 0.3 to 0.7 keV of both samples have been magnified by 30 times. (b) Typical Raman spectra of Cu foil annealed at 220 °C for 15 min, 6-month-aged graphene/copper (black), and annealed copper (red) from 200 to 800 cm^{-1}. Note that the spectrum of annealed copper has been magnified by 30 times. For both (a) and (b), the data were taken from a red-colored area (90% of the surface) for the graphene/copper sample and from a yellow-colored area (99% of the surface) for the annealed copper sample.

Significantly, the Raman peaks are *ca.* 30 times stronger for the graphene/copper sample than for the annealed copper sample. These results again suggest that more Cu_2O was formed on graphene/Cu than on the annealed Cu sample.

We note that the Raman intensity of the oxide material may be affected by the presence of a metal substrate. Specifically, near a flat metal surface, the Raman intensity of oxide may be decreased due to a decrease of electric field of incoming laser light.[25] Because this decrease of electric field occurs only near the metal surface, the overall Raman response of a copper oxide film will depend on its thickness in a nonlinear fashion. In addition, the Raman intensity of oxide could also be enhanced near a rough metal surface through the surface-enhanced Raman scattering (SERS) mechanism. In our experiment, the two samples underwent almost identical high-temperature thermal annealing. The annealing is expected to smooth the surface, and therefore we believe that

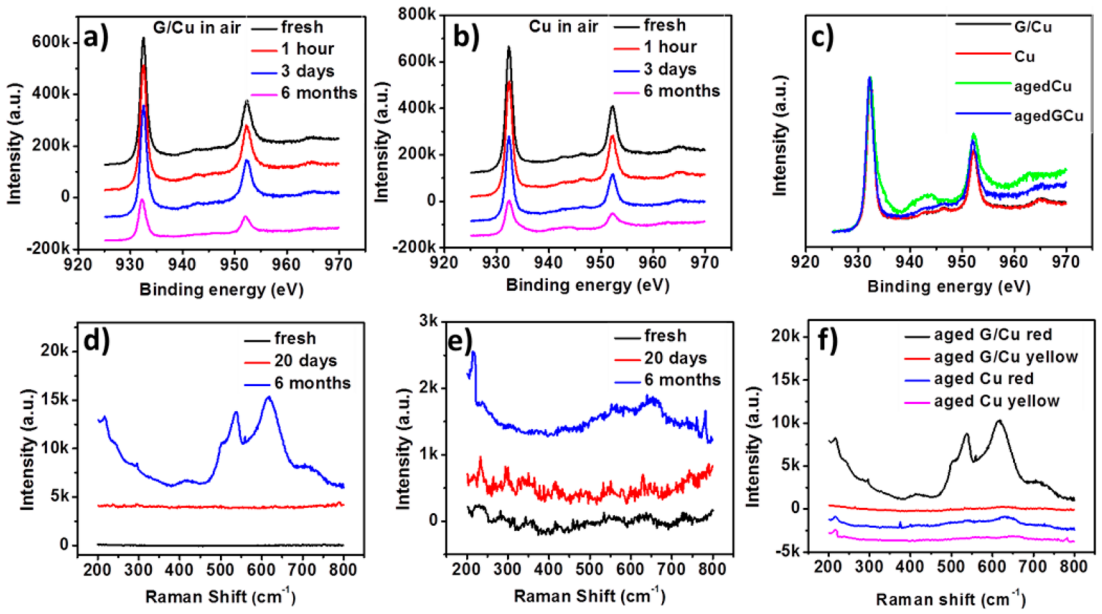

Figure 3. XPS spectra of (a) graphene-coated and (b) uncoated copper foil exposed in air at room temperature for 0 h, 1 h, 3 days, and 6 months. (c) Normalized XPS spectra of fresh and 6-month-aged copper foil with and without graphene coating. Note: the spectra of two fresh samples (red and black curves) overlap. Raman spectra of (d) graphene-coated and (e) uncoated copper foil exposed in air at room temperature for 0 days, 20 days, and 6 months, respectively. Note that the vertical scales of (d) and (e) differ by a factor of *ca.* 7. (f) Raman spectra of red and yellow regions on both 6-month-aged annealed samples.

the SERS effect will not significantly affect the relative peak intensity of the two samples. Even with these potential complications in mind, it is important to note that our Raman data are qualitatively consistent with the EDX results in that a strong Raman peak is correlated with a higher O:Cu ratio.

Oxidation Kinetics: XPS and Raman Characterization. We monitored the oxidation kinetics of copper with and without graphene coating using XPS and Raman spectroscopy. Figure 3 shows the XPS spectra of graphene/copper and annealed copper samples in the binding energy range of 920−980 eV, where the $2p_{3/2}$ and $2p_{1/2}$ peaks of copper are located. The XPS peaks of Cu(0) and Cu(I) (Cu_2O) differ by only 0.1 eV and cannot be resolved by most XPS instruments.[26] In contrast, Cu(II) species have a significant peak shift and two strong shakeup satellites at *ca.* ∼9 eV higher binding energy than the principal Cu $2p_{3/2}$ and $2p_{1/2}$ peaks.[27] We find that for both samples, the Cu XPS peak shape and binding energy remained the same within several days of their exposure in ambient air, suggesting the absence of CuO on their surfaces under these conditions. After 6 months of exposure in ambient air, the annealed copper sample exhibited a broader $2p_{3/2}$ peak (932.4 eV) and $2p_{1/2}$ peak (952.2 eV) than the graphene/copper sample; in addition, two strong satellite peaks at 942.6 and 962.7 eV, characteristic of Cu(II), were also observed (Figure 3c).[22,26−30] In contrast, the 6-month-aged graphene/copper sample showed almost the same peak width as the freshly prepared one and very small satellite peaks, both of which indicate a low concentration of Cu(II) on the surface. Further analysis by peak deconvolution showed that the atom % of Cu(II) on the surface was 6% on the 6-month-aged coated copper foil and 37% for the uncoated one (Figure S4).

Collectively, our XPS results suggest that formation of Cu(II) occurred more readily in the absence of a graphene coating than in its presence. However, in the context of assessing degree of oxidation, this result should be interpreted with caution. First of all, our XPS instrument cannot resolve a Cu(I) peak from a Cu(0) peak and therefore cannot detect oxidation if Cu_2O is the only oxidation product. Second, XPS is a surface-sensitive technique and probes only less than 10 nm within the surface.[22] The surface composition may or may not correlate with the bulk oxide composition. In fact, it was reported that exposure of copper metal to oxygen at 1000 K resulted in a thin CuO layer on top and a much thicker layer of Cu_2O underneath as the main oxidative product.[31,32]

The kinetics of copper oxidation on annealed copper and graphene/copper substrates was also investigated using Raman spectroscopy. Shown in Figure 3d,e are Raman spectra of the two samples taken right after their preparation, after 20 days of storage in air, and after 6 months of storage in air; all spectra were collected under the same conditions. Copper oxide on both samples was below the detection limit when freshly prepared and after 20 days of storage in air. The oxide-related Raman peaks became obvious only after 6 months of air exposure. As we mentioned before, the Raman intensity was typically *ca.* 30 times stronger for a 6-month-aged graphene/copper sample

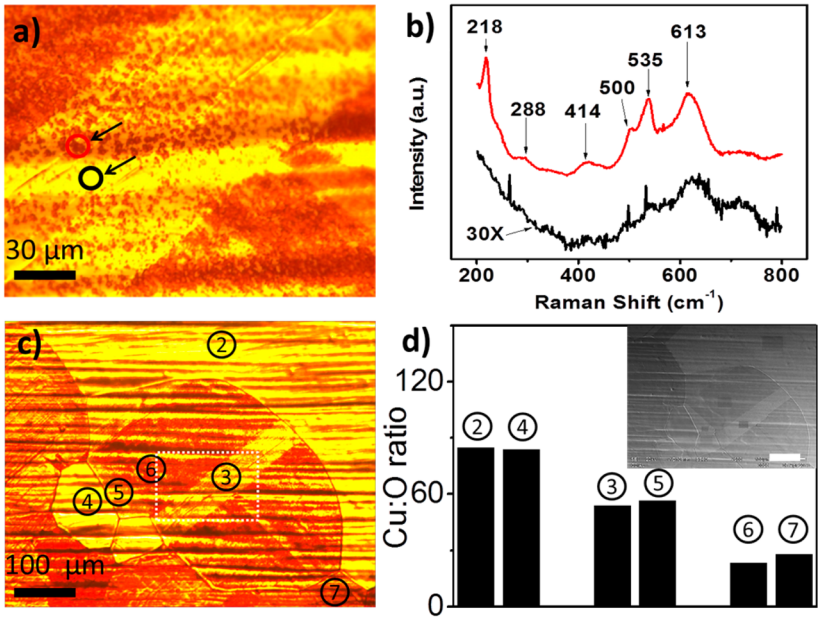

Figure 4. (a) Optical micrograph of a 6-month-aged graphene/copper sample showing red domains in a yellow background. (b) Micro-Raman spectra taken of the red and yellow areas as indicated in (a). Black and red spectra were taken from the area inside the red and black circle, respectively. (c) Optical micrograph of a 6-month-aged graphene/copper showing the different colors of the copper domains. The dotted rectangle is the same area as (a). (d) Plot of Cu:O ratio obtained by EDX on different locations indicated in (c). The inset is the SEM image of the same location as in (c). Note that for this analysis the SEM acceleration voltage (20 kV) was higher than that used in collecting EDX data of Figure 2 (10 kV); as a result, the electron beam probed a deeper sample depth and gave an overall higher Cu:O ratio in this case. The scale bar of the inset represents 100 μm.

than for a 6-month-aged annealed copper sample. Another interesting observation is that the red regions on both 6-month-aged samples gave overall more intense Raman peaks than the yellow regions (Figure 3f; also see discussion below). These data again support our conclusion that graphene enhanced long-term copper corrosion at room temperature and such oxidation was spatially inhomogeneous.

It is worth pointing out that although the surface *concentration* of Cu^{2+} measured by XPS is higher in the aged uncoated copper sample, its Raman spectrum gave a weaker CuO peak at 300 cm^{-1} when compared to the aged graphene/copper sample (Figure 2b). This seemingly contradictory observation can be explained by the fact that the aged graphene/copper sample developed a thicker oxide film. Among the two aged samples, the graphene/copper sample has a higher *amount* of CuO in the oxide film, and in addition, some of its oxide is also further away from the copper surface and therefore experiences a stronger electric field of the incoming laser; both factors translate to a stronger Raman response.

Spatial Inhomogeneity of Cu Oxidation in Graphene/Copper Sample. Additional analysis showed that the room-temperature oxidation of a copper/graphene sample was very heterogeneous at the micrometer length scale.

High-magnification optical micrographs revealed that the color change we observed on the 6-month-aged graphene/copper substrate was due to the presence of high-density micrometer-sized domains of red color (Figure 4a; also see Figure 1c,f). The colored patches we described previously (Figures 1 and S3) were due to a varying density of these red domains. If the density of these red domains was low, the yellow background will dominate the overall color of the region and the corresponding area will appear yellow to the naked eye; this is the case for the 99% of the 6-month-aged uncoated copper foil surface and only 10% of the 6-month-aged graphene/copper sample. In contrast, if the density of these red domains was high, they could form an almost continuous network and make the surface appear red (Figures 1 and S3).

Using spatially resolved micro-Raman spectroscopy, we find that the red domains corresponded to highly oxidized copper, while the yellow regions showed much reduced oxidation. Figure 4a shows an optical micrograph of a 6-month-aged copper sample that has both red and yellow regions. Figure 4b shows Raman spectra we collected in two locations: one appeared red and the other yellow. These two spots were 10 μm away, a distance significantly larger than the spot size of the focused laser beam (<1 μm) of our Raman instrument. For the Raman spectrum taken from the red region (red circle in Figure 4a), we observed peaks that can be assigned to Cu_2O and/or CuO (218, 613 cm^{-1}). In contrast, the Raman spectrum taken from the yellow region (in black circle) showed much weaker peaks (by a factor of *ca.* 30), indicating a

much smaller amount of oxidation products in this area. This correlation between color and degree of oxidation was highly reproducible (Figure S5).

A large number of Raman peaks were observed (218, 288, 414, 500, 535, and 613 cm^{-1}) in our samples. However, a definitive assignment of all these peaks is difficult because some of the Raman peaks of Cu_2O and CuO are known to show large shifts depending on the sample preparation.[33,34] While some of these peaks could be assigned to Cu_2O (613, 414, and 218 cm^{-1}) and CuO (613 cm^{-1}) with reasonable confidence,[34,35] long-term exposure of copper to ambient air could produce a wide range of corrosion products (*e.g.*, $Cu_2(OH)_3NO_3$, $Cu_2(OH)_3Cl$) that could contribute to some or all of the observed Raman peaks as well.[36]

To confirm the correlation between color change and degree of oxidation, we have also carried out spatially resolved EDX analysis of different colored regions on the 6-month-aged graphene/copper sample. We first located an area having both yellow and red regions under both optical microscope (Figure 4c) and scanning electron microscope (SEM, Figure 4d, inset). A comparison of the optical and SEM images showed that the yellow and red regions under optical microscopy appear bright and dark under SEM, respectively (Figures 4c, d-inset, and S6). We then carried out EDX analysis of six regions to obtain their Cu:O ratios, and the result is shown in Figure 4d. A clear correlation can be observed between the color of the copper surface and its degree of oxidation: the yellow regions have a higher Cu:O ratio and correspondingly a lower degree of oxidation than the red regions.

Quality of Graphene. We observed that the graphene film developed significant defects after 6 months of storage in air at room temperature. Shown in Figure S7, the graphene of a coated copper sample exhibited a negligible defect peak when freshly prepared. However, the Raman spectrum of the 6-month-aged sample showed a strong D peak, with an I_D/I_G ratio of 1.3. Surprisingly, spectra collected from both red and yellow regions showed similar I_D/I_G ratios. Another interesting observation was that the absolute Raman peak intensity of the yellow region is substantially lower than that of the red region, in some cases by a factor of almost 20. This difference in Raman intensity can be explained by the difference in oxide thickness in the two regions: in the absence of a thick oxide layer, the graphene film is in close contact with copper metal; as a result, the graphene will experience a much reduced electric field of the incident laser beam and give a weak Raman response.[25]

More interestingly, we also found that graphene developed significant mechanical damage in areas having severe Cu oxidation. Shown in Figure S8, we transferred the graphene from a 6-month-aged graphene/copper sample to a silicon wafer using polymethyl methacrylate (PMMA (Aldrich, M_w 996 000)) as the transferring agent. The PMMA was then removed by a thermal annealing at 410 °C under low pressure (~50 mTorr) for 1 h. The optical micrographs showed that the graphene covering the severely oxidized copper (red region) broke into micrometer-sized patches. In contrast, the graphene covering the less oxidized copper (yellow region) remained as a continuous film.

DISCUSSION

Our experimental results showed that graphene is a corrosion protector for short-term, high-temperature oxidation of copper and a corrosion promoter for long-term, room-temperature oxidation of copper.

Oxidation of Uncoated Copper Foil. The room-temperature oxidation of pure copper has been extensively studied in the literature. The native oxide film formed on copper (48 h of room-temperature oxidation by air) has been studied by X-ray adsorption fine structure spectroscopy (XAFS), the result of which suggested that the oxide film consists of an inner Cu_2O layer of 2.0 nm and an outer CuO layer of about 1.3 nm.[37] We believe that the same two-layer oxide was formed on our aged annealed copper foil as well: our XPS data indicated that 37% of the surface Cu was Cu(II) on the 6-month-aged annealed copper substrate, while Raman spectroscopy suggested both Cu_2O and CuO as the major oxidation products.

Oxidation of Graphene-Coated Copper Foil. An important difference between the oxidation of graphene-coated and uncoated copper foil is the much lower surface concentration (6% *vs* 37%) of Cu(II) species in the former case, as indicated by XPS. Although the lower surface concentration of Cu(II) seems to imply a limited supply of O_2 to the graphene-coated surface, the fact that the graphene-coated copper foil developed a much thicker oxide film than the uncoated one clearly suggested otherwise. Therefore we believe that hindered diffusion of O_2 cannot explain the lower concentration of surface Cu(II) species we observed on graphene-coated copper foil than on the uncoated one. In fact, the overall higher degree of copper oxidation in the presence of graphene suggested that diffusion of O_2 through a graphene coating is likely not a rate-limiting step for such low-temperature oxidation.

More interestingly, although the graphene film developed a significant amount of defects during the 6 months of air exposure, the I_D/I_G ratio of graphene was not correlated with the degree of oxidation of the underlying copper substrate. This fact suggests that although atomic level defects in graphene could lead to enhanced oxidation of underlying copper substrate at high temperature,[7] they may not necessarily do so at low temperature (*vide infra*).

Finally, it is important to note that although the graphene-coated copper sample undergoes oxidation

faster than the uncoated one, there are nevertheless regions (*e.g.*, yellow regions of Figures 1b and S3b) that did not undergo significant oxidation at all. One explanation of this observation is that the local surface structure of the copper substrate could affect its chemical reactivity as well as its adhesion to graphene, both of which could affect the kinetics of oxidation. Another possibility is that the formation of heavily oxidized domains was initiated by certain defects in graphene (*vide infra*). Knowing the exact mechanism of this observation will be critical to the long-term use of graphene as anticorrosion coatings.

Proposed Mechanism of Corrosion-Promotion Effect of Graphene. We attribute the corrosion-promotion effect of graphene to its high electrical conductivity. To understand this effect, we consider the following three key steps during the electrochemical corrosion of copper on a model surface that consists of a metallic copper substrate and a thin layer of native Cu_2O (Figure 5):

(1) Electrochemical oxidation of Cu^0 to Cu^+. This process occurs at the Cu/Cu_2O interface. The oxidation produces a free electron and a Cu^+ ion that diffuses into the Cu_2O lattice.

(2) Migration of Cu^+ and charge from the Cu/Cu_2O interface to the Cu_2O/air interface. The electron and Cu^+ generated in step 1 diffuse through the Cu_2O film to the Cu_2O/air interface, driven by the charge and ion gradient within the oxide film. It was suggested that the charge and ion migration occurred though hole transfer and cation vacancy diffusion, respectively.[38]

(3) Electrochemical reduction of O_2. This process occurs at the Cu_2O/air or Cu_2O/graphene/air interface. The reduction of O_2 requires a reducing agent and produces O^{2-} as the product. The electrochemically generated O^{2-} then incorporates into the Cu_2O lattice and combines with the incoming Cu^+ ion to form Cu_2O. A reducing agent, either free electron or Cu^+, is required for the reduction of O_2.

In the absence of a graphene coating, the electrons generated in step 1 need to migrate through the Cu_2O film to the Cu_2O/air interface. Cu_2O is a semiconductor with a band gap of *ca.* 2.0 eV,[39] and its resistivity can be as high as 10^{13} $\Omega \cdot m$.[40] The fact that there was significant concentration (37% by atom %) of Cu^{2+} on the surface of the 6-month-aged uncoated copper sample indicates that electrochemical reduction of O_2 was to some degree accompanied by the oxidation of Cu^+ to Cu^{2+}, implying that the charge migration of step 2 is slow relative to the electrochemical reduction of O_2.

In the presence of a graphene coating, the electrons generated in step 1 could be rapidly transported to the Cu_2O/graphene/air interface for O_2 reduction. In this case, O_2 likely diffuses through the cracks and defects

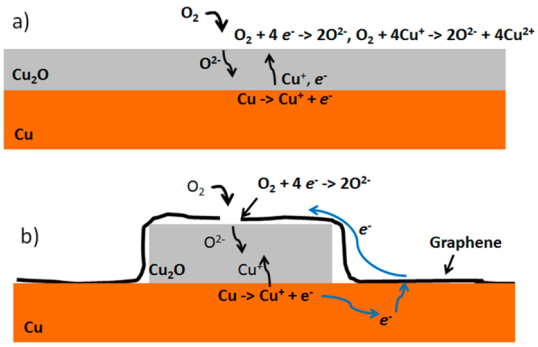

Figure 5. Electrochemical oxidation of copper in the (a) absence and (b) presence of a graphene film.

in graphene to the Cu_2O surface. Because the overall copper oxidation is spatially inhomogeneous, as long as there is still some local electrical contact between graphene and copper, electrons can easily migrate from copper to graphene, therefore enhancing the corrosion. Consistent with our proposed mechanism, we note that the surface concentration (6%) of Cu^{2+} on the aged graphene-coated copper is much lower than that of the aged copper foil. This observation is consistent with the improved availability of free electrons for O_2 reduction in the presence of graphene. As another support of this mechanism, we also observed that the oxidation of copper could be significantly slowed if the graphene/copper sample was stored in a dry environment. Shown in Figure S9, a graphene/copper sample stored in a closed vial inside a desiccator for 1 year showed less oxidation than a similar sample stored in air for 6 months. This observation is consistent with the well-known notion that reduced exposure to ambient moisture and salt aerosol slows the electrochemical corrosion process.[41]

Mechanical Damage and Defect Generation in Graphene. The graphene film of a graphene/copper sample developed significant defects after 6 months of storage in air. Specifically, the I_D/I_G ratio of the Raman spectrum increased significantly, regardless of the degree of oxidation of the underlying copper substrate. Interestingly, when transferred to a silicon wafer, the graphene covering severely oxidized copper also showed visible cracks, while no such damage was observed for graphene covering the less oxidized area. One possible explanation of these observations is that the oxidation of copper resulted in a change of surface topography. In areas having mild oxidation, the topography change resulted in only microscopic defects, while in areas having more severe oxidation, the topography change resulted in micrometer-scale cracks in the graphene. On the other hand, we also note that water can split CVD-grown graphene along its grain boundary.[42] It is entirely possible that such chemically produced defects could initiate the oxidation of copper and lead to the formation of heavily oxidized domains and subsequent crack formation in graphene. Work is under way

in our laboratory to probe the mechanistic details of the corrosion process.

CONCLUSION

Our study confirmed that graphene is a corrosion protector for short-term oxidation under aggressive chemical environments. However, graphene also promotes the long-term, room-temperature oxidation of copper. The corrosion enhancement effect of graphene is attributed to its conductive nature, which enhances the electrochemical corrosion process. Our study calls for a clear understanding of the mechanism of metal corrosion in the presence of graphene in order to enhance its long-term performance as an atomically thin anticorrosion coating.

METHODS

Preparation of Copper Substrates. *Graphene-Coated Copper Foil.* Typically, copper foil (Alfa Aesar, 99.8%, 25 μm thick) was cut into small strips (1.5 cm $\times$ 3 cm), rinsed with 1% diluted HCl, and placed at the center of a 1-in.-diameter fused quartz tube inside a tube furnace. The quartz tube was evacuated and heated to 1000 °C under a 2.0 standard cubic centimeters per minute (sccm) H_2 gas flow at a pressure of 100−110 mTorr for 30 min in order to remove any contaminants and oxides from the Cu surface. Then 20 sccm of CH_4 gas flow was introduced along with 2 sccm of H_2 gas flow at 500 mTorr and 1000 °C for another 30 min, followed by a fast cooling procedure by opening the tube furnace. The copper foil was cooled to room temperature under H_2 and CH_4 gas flow and taken out from the tube furnace.

Annealed Copper Foil (without Graphene Coating). This sample was prepared by subjecting a copper foil to the same conditions above except no CH_4 gas flow was introduced.

Optical Microscopy. Optical microscopy imaging of the copper surface was conducted using an Olympus BH2-UMA in reflectance mode with a Moticam 2000 2.0 M pixel camera (Figures 1, 4a, S3, and S5c) or a Nikon Eclipse Ti−U in reflectance mode with an Ample Scientific 3.0 M pixel camera (Figures 4c, S5a, S6a, and S6b).

Raman Spectroscopy. Room-temperature micro-Raman spectra were collected using a custom-built micro-Raman setup using a 532 nm single-longitudinal mode solid-state laser with a spot size less than 1 μm. A 40$\times$ objective (NA: 0.60) was used in all the experiments. A detailed description of the setup can be found elsewhere.[43,44] To avoid laser-induced thermal damage, the incident laser power was kept at 0.7 mW on the sample. A typical integration time was 1 h. A linear baseline correction was applied to all Raman spectra.

X-ray Photoelectron Spectroscopy. XPS measurements were carried out using a custom-built multitechnique surface analysis instrument at a base pressure of $\sim 1 \times 10^{-10}$ Torr. Spectra were collected using the Al Kα X-ray line and a Leybold-Heraeus EA-10 hemispherical energy analyzer typically operating with a bandpass of 50 eV for both survey scans (1.0 eV/step) and detailed scans (0.1 eV/step). Data analysis was carried out using XPSPEAK software[45] for both background subtraction and peak fitting.

EDX. A Philips XL-30 SEM was used to carry out EDX analysis of aged graphene/copper and annealed copper samples to provide an oxygen ratio under the same conditions (Figure 2a). EDX was performed with an acceleration voltage of 10 kV and a working distance of 10 mm.

A JEOL JSM6510LV SEM was used for imaging and EDX analysis shown in Figures 4d, S5b, and S5d. EDX was performed with an acceleration voltage of 20 kV and a working distance of 10 mm.

Conflict of Interest: The authors declare no competing financial interest.

Acknowledgment. We acknowledge financial support from the Taiho Kogyo Tribology Research Foundation, AFOSR (FA9550-13-1-0083), ONR (N000141310575), the Mascaro Center for Sustainable Innovation, and the Central Research and Development Fund of the University of Pittsburgh. We thank Y. Tang and H. Bai for their kind assistance with SEM and EDX experiments.

Supporting Information Available: Additional Figures S1−S9. This material is available free of charge *via* the Internet at http://pubs.acs.org.

REFERENCES AND NOTES

1. Chen, S. S.; Brown, L.; Levendorf, M.; Cai, W. W.; Ju, S. Y.; Edgeworth, J.; Li, X. S.; Magnuson, C. W.; Velamakanni, A.; Piner, R. D.; *et al*. Oxidation Resistance of Graphene-Coated Cu and Cu/Ni Alloy. *ACS Nano* **2011**, *5*, 1321–1327.
2. Jia, C.; Jiang, J.; Gan, L.; Guo, X. Direct Optical Characterization of Graphene Growth and Domains on Growth Substrates. *Sci. Rep.* **2012**, *2*, 707.
3. Qi, Y.; Eskelsen, J. R.; Mazur, U.; Hipps, K. W. Fabrication of Graphene with CuO Islands by Chemical Vapor Deposition. *Langmuir* **2012**, *28*, 3489–3493.
4. Nilsson, L.; Andersen, M.; Balog, R.; Laegsgaard, E.; Hofmann, P.; Besenbacher, F.; Hammer, B.; Stensgaard, I.; Hornekaer, L. Graphene Coatings: Probing the Limits of the One Atom Thick Protection Layer. *ACS Nano* **2012**, *6*, 10258–10266.
5. Luechinger, N. A.; Athanassiou, E. K.; Stark, W. J. Graphene-Stabilized Copper Nanoparticles as an Air-Stable Substitute for Silver and Gold in Low-Cost Ink-Jet Printable Electronics. *Nanotechnology* **2008**, *19*, 445201.
6. Ahn, Y.; Jeong, Y.; Lee, Y. Improved Thermal Oxidation Stability of Solution-Processable Silver Nanowire Transparent Electrode by Reduced Graphene Oxide. *ACS Appl. Mater. Interfaces* **2012**, *4*, 6410–6414.
7. Roy, S. S.; Arnold, M. S. Improving Graphene Diffusion Barriers *via* Stacking Multiple Layers and Grain Size Engineering. *Adv. Funct. Mater.* [Online Early Access] DOI: 10.1002/adfm.201203179. Published Online: Feb 26, 2013. http:// http://onlinelibrary.wiley.com/doi/10.1002/adfm.201203179/abstract (accessed July 23, 2013).
8. Kang, D.; Kwon, J. Y.; Cho, H.; Sim, J. H.; Hwang, H. S.; Kim, C. S.; Kim, Y. J.; Ruoff, R. S.; Shin, H. S. Oxidation Resistance of Iron and Copper Foils Coated with Reduced Graphene Oxide Multilayers. *ACS Nano* **2012**, *6*, 7763–7769.
9. Nayak, P. K.; Hsu, C.-J.; Wang, S.-C.; Sung, J. C.; Huang, J.-L. Graphene Coated Ni Films: A Protective Coating. *Thin Solid Films* **2013**, *529*, 312–316.
10. Kousalya, A. S.; Kumar, A.; Paul, R.; Zemlyanov, D.; Fisher, T. S. Graphene: An Effective Oxidation Barrier Coating for Liquid and Two-Phase Cooling Systems. *Corros. Sci.* **2013**, *69*, 5–10.
11. Kirkland, N. T.; Schiller, T.; Medhekar, N.; Birbilis, N. Exploring Graphene as a Corrosion Protection Barrier. *Corros. Sci.* **2012**, *56*, 1–4.
12. Prasai, D.; Tuberquia, J. C.; Harl, R. R.; Jennings, G. K.; Bolotin, K. I. Graphene: Corrosion-Inhibiting Coating. *ACS Nano* **2012**, *6*, 1102–1108.
13. Krishnamurthy, A.; Gadhamshetty, V.; Mukherjee, R.; Chen, Z.; Ren, W.; Cheng, H. M.; Koratkar, N. Passivation of Microbial Corrosion Using a Graphene Coating. *Carbon* **2013**, *56*, 45–49.
14. Serin, N.; Serin, T.; Horzum, S.; Celik, Y. Annealing Effects on the Properties of Copper Oxide Thin Films Prepared by Chemical Deposition. *Semicond. Sci. Technol.* **2005**, *20*, 398–401.
15. Topsakal, M.; Sahin, H.; Ciraci, S. Graphene Coatings: An Efficient Protection from Oxidation. *Phys. Rev. B* **2012**, *85*, 155445.

16. Hihara, L. H.; Latanision, R. M. Corrosion of Metal-Matrix Composites. *Int. Mater. Rev.* **1994**, *39*, 245–264.
17. Bobić, B.; Mitrović, S.; Babić, M.; Bobić, I. Corrosion of Metal-Matrix Composites with Aluminium Alloy Substrate. *Tribol. Ind.* **2010**, *32*, 3–11.
18. Hihara, L. H.; Latansion, R. M. Localized Corrosion Induced in Graphite/Aluminum Metal-Matrix Composites by Residual Microstructural Chloride. *Corrosion* **1991**, *47*, 335–340.
19. Li, X. S.; Cai, W. W.; An, J. H.; Kim, S.; Nah, J.; Yang, D. X.; Piner, R.; Velamakanni, A.; Jung, I.; Tutuc, E.; *et al*. Large-Area Synthesis of High-Quality and Uniform Graphene Films on Copper Foils. *Science* **2009**, *324*, 1312–1314.
20. Goldstein, J. I. Electron Beam-Specimen Interaction. In *Practical Scanning Electron Microscopy*; Goldstein, J. I., Yakowitz, H., Ed.; Springer: New York, USA, 1975; pp 49−94.
21. Chou, M. H.; Liu, S. B.; Huang, C. Y.; Wu, S. Y.; Cheng, C. L. Confocal Raman Spectroscopic Mapping Studies on a Single CuO Nanowire. *Appl. Surf. Sci.* **2008**, *254*, 7539–7543.
22. Gan, Z. H.; Yu, G. Q.; Tay, B. K.; Tan, C. M.; Zhao, Z. W.; Fu, Y. Q. Preparation and Characterization of Copper Oxide Thin Films Deposited by Filtered Cathodic Vacuum Arc. *J. Phys. D: Appl. Phys.* **2004**, *37*, 81–85.
23. Irwin, J. C.; Chrzanowski, J.; Wei, T.; Lockwood, D. J.; Wold, A. Raman-Scattering from Single-Crystals of Cupric Oxide. *Phys. C* **1990**, *166*, 456–464.
24. Niaura, G. Surface-Enhanced Raman Spectroscopic Observation of Two Kinds of Adsorbed OH^- Ions at Copper Electrode. *Electrochim. Acta* **2000**, *45*, 3507–3519.
25. Greenler, R. G.; Slager, T. L. Method for Obtaining the Roman Spectrum of a Thin Film on a Metal Surface. *Spectrochim. Acta, Part A* **1973**, *29*, 193–201.
26. Dube, C. E.; Workie, B.; Kounaves, S. P.; Robbat, A.; Aksu, M. L.; Davies, G. Electrodeposition of Metal Alloy and Mixed-Oxide Films Using a Single-Precursor Tetranuclear Copper-Nickel Complex. *J. Electrochem. Soc.* **1995**, *142*, 3357–3365.
27. Poulston, S.; Parlett, P. M.; Stone, P.; Bowker, M. Surface Oxidation and Reduction of CuO and Cu_2O Studied Using XPS and XAES. *Surf. Interface Anal.* **1996**, *24*, 811–820.
28. Yoon, C.; Cocke, D. L. Evidence for Electron-Transfer Control of Oxygen Incorporation into Bulk Copper. *J. Electrochem. Soc.* **1987**, *134*, 643–644.
29. Espinos, J. P.; Morales, J.; Barranco, A.; Caballero, A.; Holgado, J. P.; Gonzalez-Elipe, A. R. Interface Effects for Cu, CuO, and Cu_2O Deposited on SiO_2 and ZrO_2. XPS Determination of the Valence State of Copper in Cu/SiO_2 and Cu/ZrO_2 Catalysts. *J. Phys. Chem. B* **2002**, *106*, 6921–6929.
30. Biesinger, M. C.; Lau, L. W. M.; Gerson, A. R.; Smart, R. S. C. Resolving Surface Chemical States in XPS Analysis of First Row Transition Metals, Oxides and Hydroxides: Sc, Ti, V, Cu and Zn. *Appl. Surf. Sci.* **2010**, *257*, 887–898.
31. Mimura, K.; Lim, J.-W.; Isshiki, M.; Zhu, Y.; Jiang, Q. Brief Review of Oxidation Kinetics of Copper at 350 to 1050 °C. *Metall. Mater. Trans. A* **2006**, *37*, 1231–1237.
32. Zhu, Y. F.; Mimura, K.; Isshiki, M. Oxidation Mechanism of Copper at 623−1073 K. *Mater. Trans.* **2002**, *43*, 2173–2176.
33. Shinde, S. L.; Nanda, K. K. Facile Synthesis of Large Area Porous Cu_2O as Super Hydrophobic Yellow-Red Phosphors. *RSC Adv.* **2012**, *2*, 3647–3650.
34. Texier, F.; Servant, L.; Bruneel, J. L.; Argoul, F. *In Situ* Probing of Interfacial Processes in the Electrodeposition of Copper by Confocal Raman Microspectroscopy. *J. Electroanal. Chem.* **1998**, *446*, 189–203.
35. Hurley, B. L.; McCreery, R. L. Raman Spectroscopy of Monolayers Formed from Chromate Corrosion Inhibitor on Copper Surfaces. *J. Electrochem. Soc.* **2003**, *150*, B367–B373.
36. Bertolotti, G.; Bersani, D.; Lottici, P. P.; Alesiani, M.; Malcherek, T.; Schluter, J. Micro-Raman Study of Copper Hydroxychlorides and other Corrosion Products of Bronze Samples Mimicking Archaeological Coins. *Anal. Bioanal. Chem.* **2012**, *402*, 1451–1457.
37. Keil, P.; Lutzenkirchen-Hecht, D.; Frahm, R. Investigation of Room Temperature Oxidation of Cu in Air by Yoneda-XAFS. *AIP Conf. Proc.* **2007**, *882*, 490–492.
38. Kear, G.; Barker, B. D.; Walsh, F. C. Electrochemical Corrosion of Unalloyed Copper in Chloride Media - A Critical Review. *Corros. Sci.* **2004**, *46*, 109–135.
39. Hara, M.; Kondo, T.; Komoda, M.; Ikeda, S.; Shinohara, K.; Tanaka, A.; Kondo, J. N.; Domen, K. Cu_2O as a Photocatalyst for Overall Water Splitting under Visible Light Irradiation. *Chem. Commun.* **1998**, 357–358.
40. Tapiero, M.; Zielinger, J. P.; Noguet, C. Electrical Conductivity and Thermal Activation Energies in Cu_2O Single Crystals. *Phys. Status Solidi A* **1972**, *12*, 517–520.
41. Dante, J. F.; Kelly, R. G. The Evolution of the Adsorbed Solution Layer during Atmospheric Corrosion and Its Effects on the Corrosion Rate of Copper. *J. Electrochem. Soc.* **1993**, *140*, 1890–1897.
42. Feng, X. F.; Maier, S.; Salmeron, M. Water Splits Epitaxial Graphene and Intercalates. *J. Am. Chem. Soc.* **2012**, *134*, 5662–5668.
43. Surwade, S. P.; Li, Z.; Liu, H. Thermal Oxidation and Unwrinkling of Chemical Vapor Deposition-Grown Graphene. *J. Phys. Chem. C* **2012**, *116*, 20600–20606.
44. Zhao, S. C.; Surwade, S. P.; Li, Z. T.; Liu, H. T. Photochemical Oxidation of CVD-Grown Single Layer Graphene. *Nanotechnology* **2012**, *23*, 355703.
45. UK Surface Analysis Forum, http://www.uksaf.org/software.html (accessed: April 1, 2013).